Jour. Fac. Sci., Hokkaido Univ., Ser. IV,
vol. 22, no. 2, Aug., 1987, pp. 259-275.

A PALEOMAGNETIC RECONNAISSANCE OF SOME LATE PRECAMBRIAN TO EARLY PALEOZOIC ROCKS OF TANSEN AREA, LESSER HIMALAYA, NEPAL

by

Pitambar Gautam

(with 13 text-figures and 3 tables)

Abstract

For a preliminary paleomagnetic research on Late Precambrian to Early Paleozoic rocks in the Tansen area (West Central Nepal) carbonate, sandstone, quartzite and slate were collected from 30 sites at 4 localities. Detailed analyses of magnetic remanence were made using alternating field and thermal demagnetization techniques. Most of the specimens were found to be weakly magnetized (intensities of 10^{-7} emu/cc, in order). Three magnetic components have been distinguished: (1) a predominant secondary component of recent origin, which represents a larger portion of the magnetization intensity in weakly magnetized specimens and thus hinders the separation of primary components. (2) another component (probably secondary), which yields a mean direction: $D=320°$, $I=10°$, $a_{95}=21°$ (before bedding correction) restricted only to purple slate varieties of Ramdighat Formation, and (3) a probably characteristic mean direction: $D=350°$, $I=-45°$, $a_{95}=15°$ derived from carbonate rock specimens of Kerabari Formation. This direction gives a virtual geomagnetic south pole position at 36°S/95°E.

Introduction

During the last three decades an increasing number of paleomagnetic data have been gathered from the Himalayan region and the Indian Subcontinent. The data have been used to construct an apparent polar wander path for the region and to interpret them in terms of large-scale drifting of the Indian fragment of the Gondwanaland. Furthermore, efforts have been made to use the data to predict the time of the inferred collision of India with Asia and to evaluate the post-collisional extent of the former. However, the rocks from Nepal Himalaya have been remained hitherto little studied paleomagnetically except for a few cases. Bingham & Klootwijk (1980) and Klootwijk & Bingham (1980) described the paleomagnetism of the fossiliferous sedimentary rocks of Late Paleozoic and Mesozoic age in the Tibetan Tethys Zone, the Thakkhola region. Tokuoka & Yoshida (1984) reported the magnetic stratigraphy of Tertiary Siwalik rocks in the Subhimalayas. Works by Yamanaka et al. (1982), Yoshida & Igarashi (1984) and Yoshida et al. (1984) concerning magnetostratigraphy are restricted to Neogene to Quaternary deposits of the Pokhara valley, the Kathmandu valley and the Takmar Series, respectively. There exists only one paper (Yoshida & Sakai, 1984) on the paleomagnetism of Nepalese Lesser Himalayan rocks, where preliminary studies of Late Paleozoic to Cenozoic rocks of the Tansen Group have been carried out.

It is true that not much attention is paid to the paleomagnetic investigations of the

Contribution from the Department of Geology and Mineralogy, Faculty of Science, Hokkaido University, No. 1924.

Lesser Himalayan sediments. Reliable paleomagnetic data acquisition and their interpretation from the weakly magnetized rocks becomes more difficult due to the following reasons: (1) lack of stratigraphic control because there are very few fossil findings and almost no radioactive age determinations. (2) relatively high degree of weathering which the rocks have undergone, and (3) complex structure due to intense folding, faulting and thrusting as well as metamorphism.

However, a careful examination of the rocks should be reasonable before rejecting them for paleomagnetic studies. The present work is aimed to investigate the suitability of some Lesser Himalayan rocks for further paleomagnetic research. It would be of great importance if the paleomagnetism in the Nepal Lesser Himalaya can be applied for assigning the age to the rock units by correlating them with other paleomagnetically well-known areas in the Himalayan region. For this purpose, the rocks from Kali Gandaki Supergroup (Sakai 1985) in Tansen area, were selected. The selection is basically due to two factors: the availability of detailed geological map and lithostratigraphic columns (Sakai, 1983, 1985) on the one hand, and some positive indications on suitability for paleomagnetic studies of the overlying rocks from Tansen Group (Yoshida & Sakai, 1984) on the other.

General geological setting

The territory of present study is located around the town of Tansen in Central West Nepal. The area belongs to the southern part of the Lesser Himlayan zone lying mainly between the Main Boundary Thrust (MBT) in the south and middle reaches of the Kali Gandaki river in the north. Most of the previous geological works (Frank & Fuchs, 1970; Fuchs & Frank, 1970; Hashimoto et al., 1973; Fuchs, 1980; Mascle, 1980; Sharma, 1980; Arita et al., 1982; Sharma et al., 1984 and others) dealing with the area have been carried out on regional scale with emphasis on lithostratigraphic division and structural zoning. More detailed works (Arita & Yoshida, 1982; Sakai, 1983, 1984, 1985) carried out recently make possible to discuss geology of the area in detail. The following is a brief geological description of the study area based on these recent works.

Tansen area is divided into two major stratigraphic units: the Tansen Group and the Kali Gandaki Supergroup. The Tansen Group consists mainly of clastic sediments of Late Carboniferous to Early Miocene age. The Kali Gandaki Supergroup underlies the Tansen Group disconformably. This supergroup attains a thick sequence (>10 km in thickness) of non-to weakly-metamorphosed terrigeneous and carbonaceous rocks, deposited mainly under arid climates and shore-line environment. Among the reported organic remains are stromatolites and some tiny plant remains in carbonaceous or coaliferous beds from some horizons. So, based mainly on lithostratigraphic comparison of these rocks with rock formations in other regions (Nawakot complex in Central Nepal, the Vindhyans in the Indian Shield, Kumaon Himalayan rocks etc.) and the fact that these rocks underlie the glacial diamictites of the Sisne Formation, the lowest member of the Tansen Group, assigned Permo-Carboniferous age, the group is

given Late Precambrian to Early Paleozoic age. It will be worth noticing that there are uncertainties concerning the upper age limit of the group and are discussed in detail in the papers mentioned above.

Three structural belts are recognized in the area: the Tansen Synclinorium, Angha Khola recumbent fold belt and Khoraidi fold belt from south to north respectively. The first and second of them are separated by the so-called Northern Boundary Fault (NBF) while the Ramdi Fault separates the second and the third. The Tansen Group embraces the doubly plunging Tansen Synclinorium and is covered in the central part by Palpa klippe. This klippe is believed to be formed due to the overthrusting of the Angha Khola recumbent fold belt upon the synclinorium. In the southern part of Palpa klippe, the Tansen Group forms an imbricate structure.

A geological sketch map and the simplified lithostratigraphic description is presented in Text-figs. 1 & 2.

Sampling

Oriented block samples were collected from 4 localities (30 sites) using a magnetic compass. The samples belong to the middle and upper groups of the Kali Gandaki Supergroup. Two or three blocks were collected from each site. Sampling localities, which are shown in the sketch map (Text-fig. 1) are as follows:

1) Baugha Pokharathok area (sites PA 1 — PA16)

The area is characterized by continuously outcropping sequence ranging from the Chappani Formation to the Ramdighat Formation within a small area. The sequence is

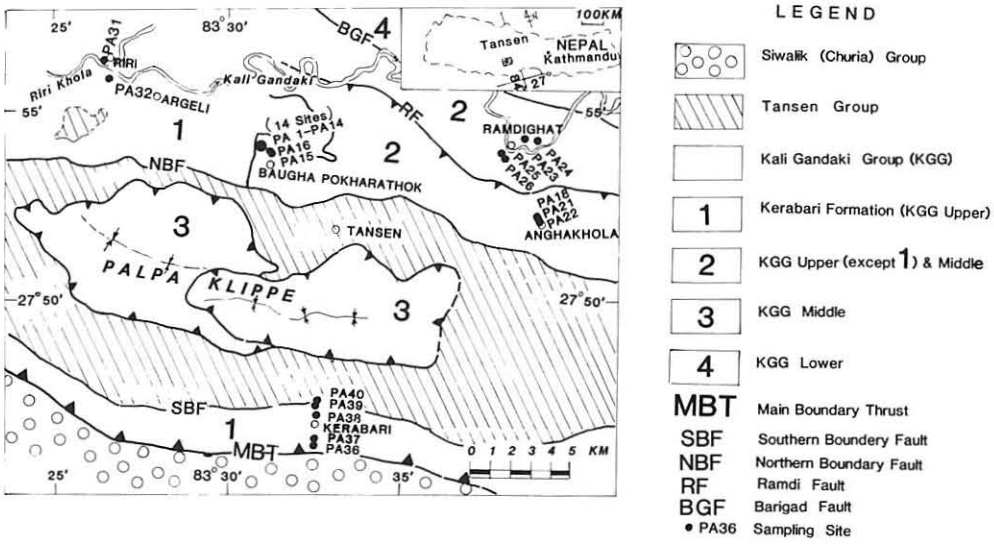

Text-fig. 1 Geological sketch map (after Sakai, 1983, 1985) of the area studied showing sampling sites.

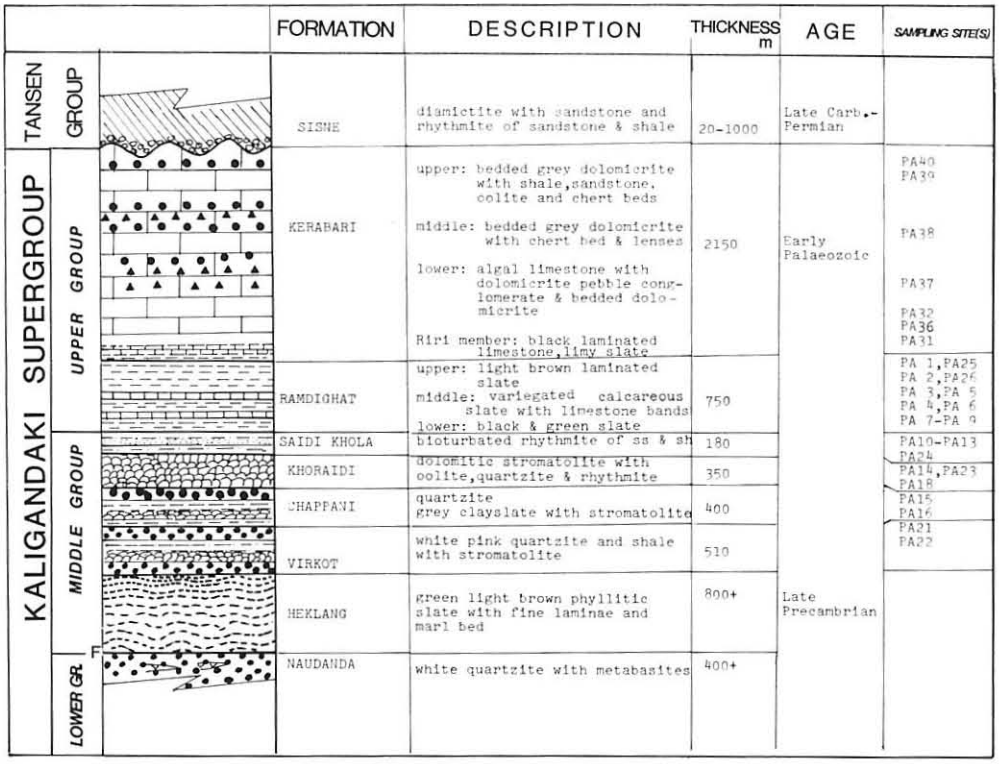

Text-fig. 2 Chart showing lithological description of strata (modified after Sakai, 1985) and stratigraphic distribution of paleomagnetic sampling sites.

thrust up on the topmost bed of the Kerabari Formation and, is overturned everywhere (Sakai, 1985). Sampling was started from the downstream (approx. height 1220m) of Dharadi Khola ("Khola" in Nepali is a general term for stream, rivulet or a small river) in the western slope of the Pokharathok ridge, where the first exposure of dark gray calcareous slate (Ramdighat Formation) starts. Sampling was continued upstream until the exposure of yellowish brown sandstone with stromatolitic dolomite intercalations and alternating with strongly bioturbated shale (site PA14, approx. height 1490m). Text-fig. 3 is the simplified route map along Dharadi Khola showing the sampling sites PA1 to PA14. Sites PA15 and PA16 are situated at the outcrops of slightly metamorphosed phyllitic slate (Chappani Formation) in the eastern slope of the ridge.

2) Angha Khola — Ramdighat area (sites PA18 and PA21—PA26)

First 3 sites belong to a reverse sequence exposed along the lower reaches of the Angha Khola. Site PA18 belongs to the Khoraidi dolomite approximately 200m upstream from the junction of the Angha Khola and the Muslang Khola. Site PA21 is an exposure of thick bedded massive pinkish white quartzose sandstone with rare inter-

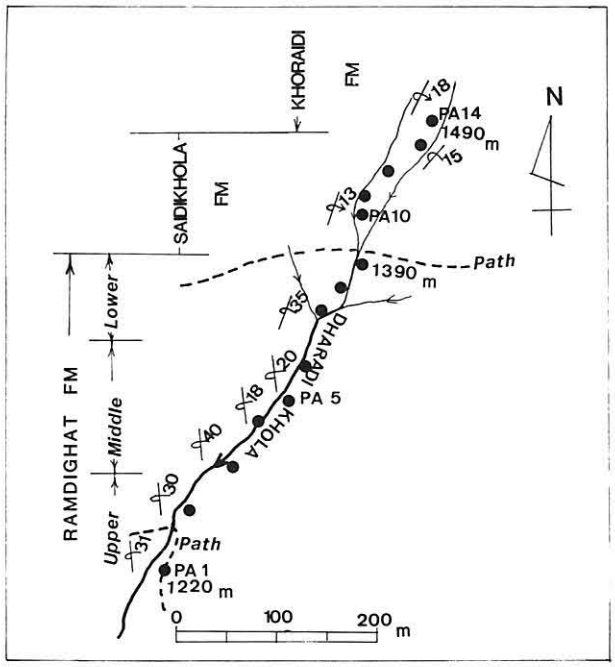

Text-fig. 3 Simplified route map along Dharadi Khola showing sampling sites from PA1 to PA14 (solid circles).

calation of greenish gray shale (Virkot Formation) located just 150m downstream from the lower end of the Angha Khola Bazaar. An exposure of reddish brown quartzite situated immediately after the end of the bridge on the right bank of the river corresponds to site PA22.

An exposure of stromatolitic dolomite alternating with sandstone forming a cliff along the highway 300m east of Ramdighat was selected as site PA23. The stromatolites occur to be upset, which indicates overturning of the beds. Site PA24 corresponds to the first exposure of thinly laminated phyllitic slate, to the east of the previous site along the highway.

Sites PA25 and PA26 were placed at outcrops of black slate (Ramdighat Formation) along the motor road south of the Upsa bridge.

3) Riri-Argeli area (sites PA31—PA32)

An exposure of gray thinly laminated calcareous slate 150m upslope from the Riri Khola bridge, on motorable road was seleced as site PA31. Samples of thick bedded platy limestone at Argeli form site PA32.

4) Kerabari area (sites PA36—PA40)

Five sites were sampled along the highway in the vicinity of Kerabari village, where a complete section corresponding to the Kerabari Formation is exposed. Sites PA36 and PA37 show undulated bedding features probably caused by the activity of Main Boundary Thrust. Site PA37 exhibits overturned bedding.

Stratrigraphic positions of the sampling sites are shown in Text-fig. 2.

Laboratory measurements

Normally, two cylindrical specimens (2.54cm in diameter, 2.5cm in length) were drilled from each sample. The remanent magnetization was measured using a Schonstedt SSM1A spinner magnetometer. All measurements were carried out at the paleomagnetic laboratory of Hokkaido University.

NRM Measurements

The initial NRM data are presented in the Table 1. The mean NRM intensity for sites shows a variation between 1.5×10^{-5} to 3.7×10^{-8} (emu/cc), most of samples having intensity of 10^{-7} order. Some rock types were found to be so weak that no reliable measurement was possible (e.g., black slate of Ramdighat Formation). Except the sandstone from site PA10 the reddish purple slate specimens from the Ramdighat Formation possess highest intensities (10^{-6} emu/cc). Sites PA4 and PA5 were splitted up into two subgroups owing to lithological differences and largely differing magnetic directions.

Demagnetization studies

Alternating field (AF) demagnetization studies were carried out on an apparatus, which utilizes a 400 Hz alternating field, without specimen rotation. At least one specimen from each site was demagnetized in increasing peak fields of 100, 200, 300, 400, 500 and 530 Oersteds. In some cases, however specimens could not be subjected to all these steps owing to the rapid decay of intensities reaching to the noise level of the instrument.

A visual analysis to assess the directional stability and coercivity spectrum of each specimen was done using orthogonal component plots (Zijderveld, 1967), normalized intensity decay curves, and Schmidt's equal-area net plots of directional changes for successive demagnetization steps. On the basis of such analysis the following three groups of specimens were distinguished:

First group of specimens which show that relatively soft components become reduced after 200—300 Oersted treatment reaching a relatively stable direction. The normalized intensity curves for these specimens show that about 50% of intensity reduces during AF treatment up to 500 Oersted (e.g., specimens PA 6-1A, PA15-3A and PA31-1B: see Text-fig. 4).

Second group of specimens shows elimination of unstable soft components around 300 Oersted. At the same time, 60—90% of initial intensity becomes reduced. Further treatment in higher fields leads to the decrease in intensity to the noise level of the instrument (e.g., specimens from sites PA38, PA39 and PA40: see Text-fig. 5).

And, the third group of specimens exhibiting a "hard" component, where less than 10% of the initial intensity becomes reduced during AF treatment up to 550 Oersted without any notable changes in directions (e.g., specimens from sites PA10 and PA14: see Text-fig. 6). The same is true for purple slate specimens from the Ramdighat Formation.

Table 1 Natural remanent magnetization (NRM) directions* of sites

Site	n (N)	D (°)	I (°)	k	a_{95} (°)	Intensity ($\times 10^{-9}$ emu/cc)	Rock type**	Bedding*** (Strike/Dip)
PA 1	3	356	50	11	24	78	gray calc. sl.	N 8W 31NE (O)
PA 2	3	357	46	63	10	320	gray calc. sl.	N 8W 35NE (O)
PA 3	3 (6)	348	20	58	7	3400	purple sl.	N15W 38NE (O)
PA 4 (A)	2 (3)	313	10	45	14	1100	purple sl.	N15W 18NE (O)
PA 4 (B)	1 (2)	347	40	—	—	3200	green sl.	N15W 18NE (O)
PA 5 (A)	2	316	7	103	9	5600	purple sl.	N14W 20NE (O)
PA 5 (B)	1	326	34	—	—	2600	green sl.	N14W 20NE (O)
PA 6	2 (3)	334	44	120	7	250	green calc. sl.	N 7W 30NE (O)
PA 7	2	8	46	—	—	160	green sl.	N16E 35SE (O)
PA 8	1	332	37	—	—	37	black sl.	N48E 20SE (O)
PA10	2 (3)	0	47	169	6	15000	ss., sl.	0N 20 E (O)
PA11	2 (3)	16	53	17	19	870	ss.	N30E 13SE (O)
PA12	2 (3)	339	38	40	15	780	silty sl.	N10E 34SE (O)
PA13	1	16	34	—	—	530	ss.	N40E 15SE (O)
PA14	2 (4)	357	40	664	2	3600	ss.	N38E 18SE (O)
PA15	2	346	44	—	—	320	phyllitic sl.	N10E 54SE (A)
PA16	3	345	41	47	11	820	phyllitic sl.	N21E 55SE (A)
PA18	2 (3)	333	45	107	7	240	ss., qtz.	N85W 18SW (O)
PA22	2	48	36	—	—	220	qtz.	N68E 30SE (O)
PA23	3 (4)	11	38	53	9	130	dol., ss.	N20E 20SE (O)
PA24	3	157	84	4	37	440	sl.	N10W 30NE (A)
PA31	2	357	47	—	—	86	black calc. sl.	N60W 35NE (A)
PA32	2	354	52	—	—	98	ls.	N62W 30SW (A)
PA36	2	329	50	—	—	64	gray ls.	N85E 45NW (N)
PA37	2	346	52	—	—	140	ls.	N85E 83SE (O)
PA38	2 (3)	349	26	75	9	160	dol., ls	N83E 50NW (N)
PA39	3 (7)	342	48	18	12	200	dol., ls.	N84W 85NE (N)
PA40	2 (3)	13	67	5	35	280	calc. ss.	N65W 85NE (N)

* n and N are the number of samples and specimens, respectively; D is the declination of the magnetization direction, measured eastwards from north; I is the inclination of the magnetization direction, downwards positive, upwards negative; a_{95} is the semi-angle of cone of 95% confidence; k is the estimate of the Fisher's precision parameter.
(Directions not corrected for bedding)

** Abbreviations: calc. = calcareous, sl. = slate, ss. = sandstone, qtz. = quartzite, dol. = dolomite, ls. = limestone

*** Bedding: (N) = Normal, (O) = Overturned, (A) = Uncertain

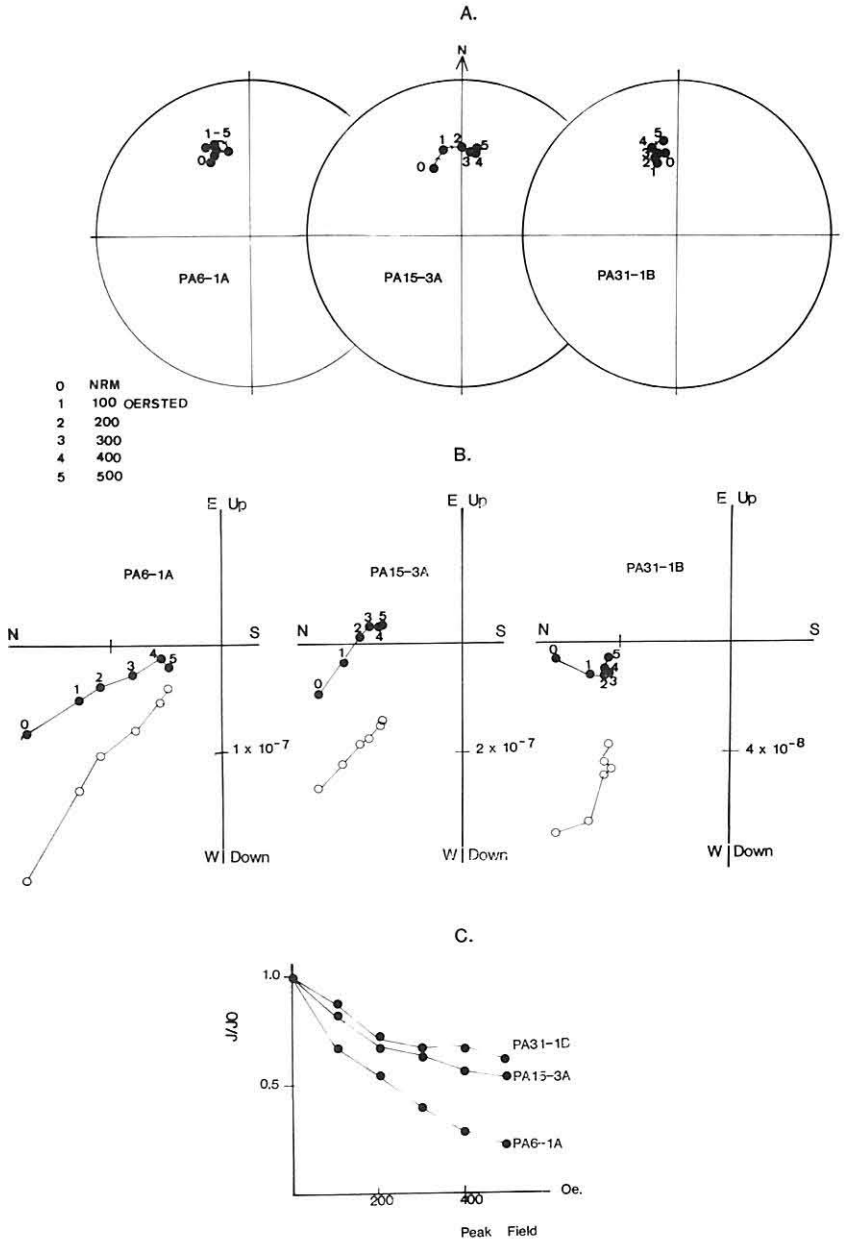

Text-fig. 4 Results of stepwise AF demagnetization of specimens PA6-1A, PA15-3A and PA31-1B.

A. Vector migration plots. Solid (open) circles denote the lower (upper) hemisphere projections of magnetization vector on a Schmidt's equal-area net.

B. Orthogonal projection diagrams. Projections of the end-points of the resultant magnetic vector during successive demagnetization. Solid and open circles represent the projections on the horizontal and north-south vertical planes respectively. Units along axes are given in emu/cc. Numbers 0,1,2,3,4,5, besides the circles in **A.** and **B.** denote the peak alternating field values as shown in the middle left corner.

C. Normalized intensity response curves.

(Results not corrected for bedding)

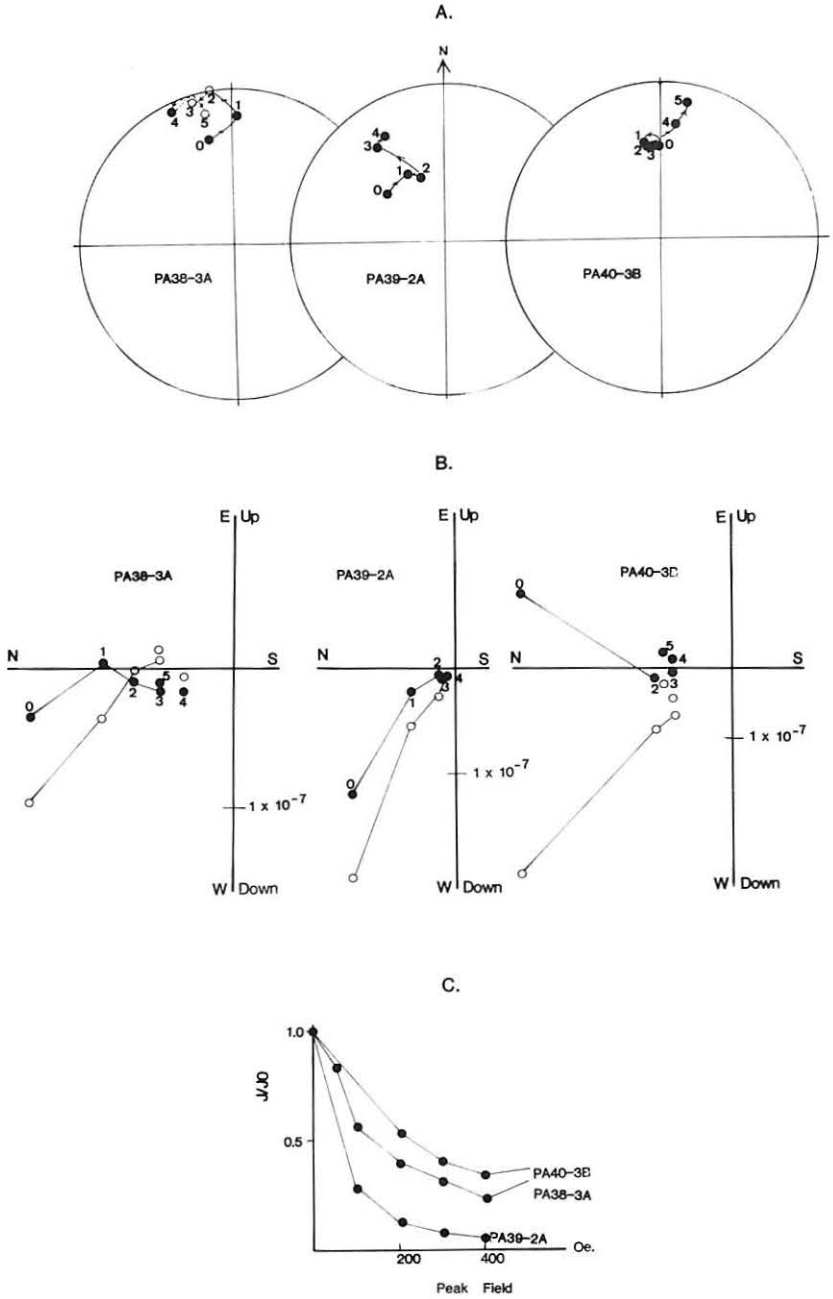

Text-fig. 5 Results of stepwise AF demagnetization of specimens PA38-2A, PA39-2A and PA40-3B. Conventions same as in Text-fig. 4.

Thermal demagnetization (THD) was carried out on pilot specimens from each formation. Progressive heating of the pilot specimens was done in 6—10 steps up to a maximum temperature of 550(°C) in air. The remanent magnetization was measured after cooling to the room temperature after each successive heating step. The heating-cooling process was carried out in a magnetically field-free space. The same type of analysis applied for AF demagnetization data was made for THD data. It was established that thermal treatment is not applicable to first and second groups of specimens (mentioned above) due to rapid decay of the magnetization intensity to the noise-level of the instrument soon after one or two heating steps. Only third group specimens were found suitable for THD studies because of their relatively higher initial intensities. The orthogonal component plots for the purple slate specimens (sites PA3, PA4(A) and PA5(A)) showed that a relatively stable direction is reached after 300°C (Text-fig. 7). Some of the specimens exhibited "hard" direction during THD (e.g., specimen PA10-3B: see Text-fig. 8).

Based on the results of demagnetization studies on pilot specimens, the rest of the specimens were subjected to either AFD (optimum peak fields of 200 and 300 Oersted) or THD (optimum temperature of 300°C), depending on their magnetic behavior during cleaning. Table 2 is the listing of results or the magnetic cleaning studies.

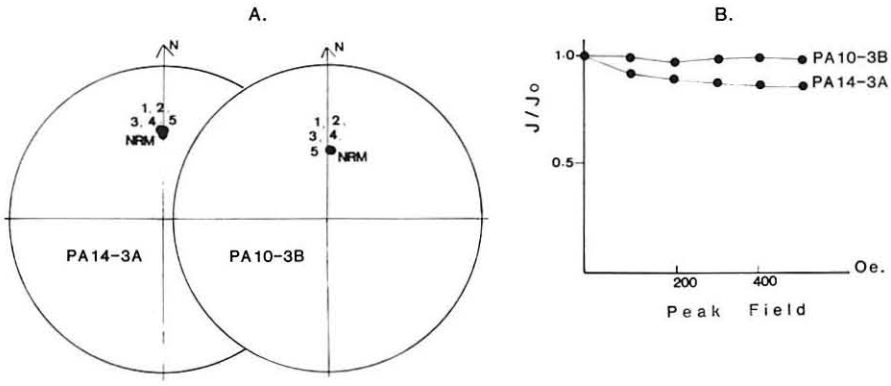

Text-fig. 6 Results of stepwise AF demagnetization of specimens PA10-3B and PA14-3A.
A. Vector migration plots.
B. Normalized intensity response curves.
Other symbols as in Text-fig. 4

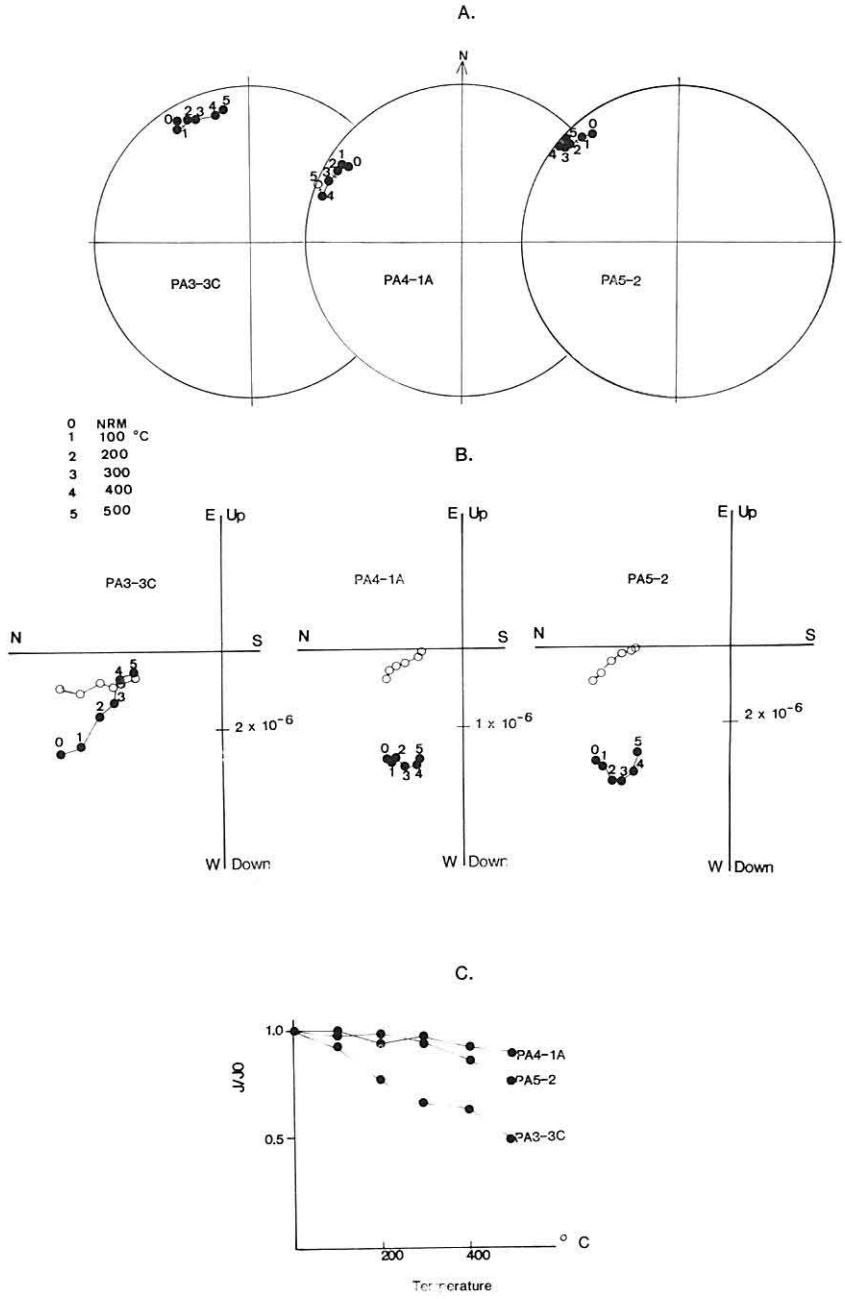

Text-fig. 7 Results of progressive thermal demagnetization of specimens PA3-3C, PA4-1A and PA5-2. The numbers 0,1,2,3,4,5 besides the projection points denote the heating temperatures as shown in the middle left corner. Other conventions as in Text-fig. 4.

Table 2 Magnetization directions of sites after demagnetization*

Site	AFD (Oe)	THD (°C)	(Bedding not corrected) D (°)	I (°)	k	a_{95}(°)	(Bedding corrected) D_c(°)	I_c(°)	k	a_{95}(°)
PA 1	300		354	51	17	19				
PA 2	300		14	51	13	21				
PA4 (B)		300	343	44	—	—				
PA 6	200		337	33	90	8				
PA10	200		4	47	216	5				
PA11	200		19	51	—	—				
PA13	100		22	43	—	—				
PA18	200		333	45	107	7				
PA23	200		3	32	72	8				
PA31	200		347	46	—	—				
PA32	200		353	36	—	—				
PA 3		300	346	14	77	9	335	−11		
PA4 (A)		300	304	9	10	24	22	−21		
PA5 (A)		300	312	7	—	—	16	−18		
Mean (3 sites)			320	10	13	21	4	−18	10	24
PA36	300		313	3	—	—	305	−24		
PA37	300		259	65	—	—	330	−4		
PA38	300		0	6	4	40	2	−44		
PA39	300		336	28	19	12	326	−47		
PA40	300		2	41	66	9	2	−40		
Mean (5 sites) / PA36-PA40 /			334	32	4	29	335	−34	9	20
Mean (3 sites) / PA38-PA40 /			352	25	13	21	350	−45	28	15

* The number of samples and specimens for site is same as in Table 1.
AFD = Alternating Field demagnetization, Peak field value (Oersted)
THD = Thermal demagnetization, Temperature (degree Celcius)
Other conventions, same as in Table 1.

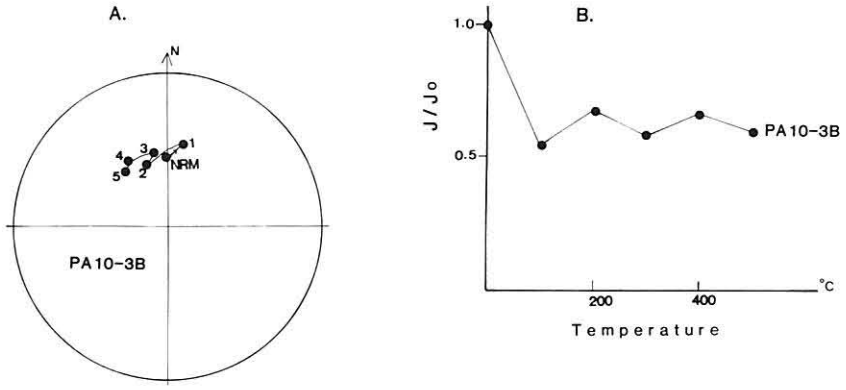

Text-fig. 8 Results of progressive thermal demagnetization of a specimen PA10-3B.
A. Vector migration plot.
B. Normalized intensity response curve.
Other conventions as before.

Interpretation of results

The NRM directions from the sites have NNW to NNE declinations and moderately steep downward inclinations exhibiting only normal polarity. An equal-area projection of these directions (Text-fig. 9) shows a clustering, which is very close to the axial geocentric dipole field direction at present for Tansen (D = 0°, I = 47°). After cleaning, for most of the sites, neither the grouping of mean directions for specimens within a site is improved nor the site-mean directions do show any significant departure from the NRM site-mean directions (Text-fig. 10). Such a behavior can be interpreted in terms of largely overprinting or complete remagnetization of the rocks in the recent magnetic field. This is believed to be due to the viscous nature of the remanence or the consequence of weathering in these rocks.

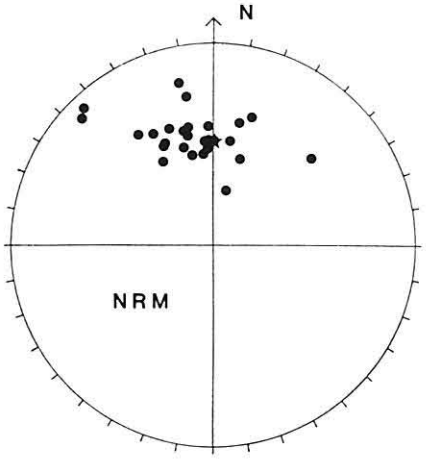

Text-fig. 9 Schmidt's equal-area projection of NRM directions of all sites measured. Solid circles denote projections in lower hemisphere. Star indicates the axial geocentric dipole field direction (I = 47°) at present for Tansen. For data, see Table 1. Directions not corrected for bedding.

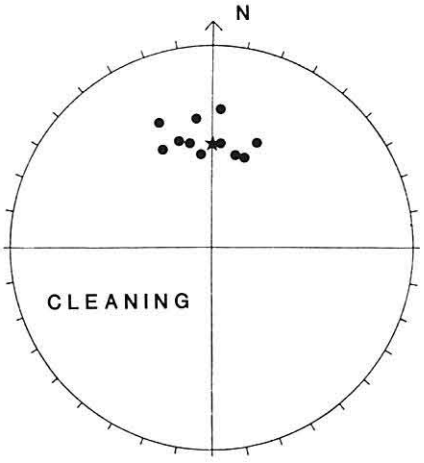

Text-fig. 10 Schmidt's equal-area projection of mean directions for sites PA1, PA2, PA4(B), PA6, PA10, PA11, PA13, PA18, PA23, PA31, and PA32 (11 sites, Table 2) after demagnetization. Bedding correction not applied. Plotting conventions same as in Text-fig. 9.

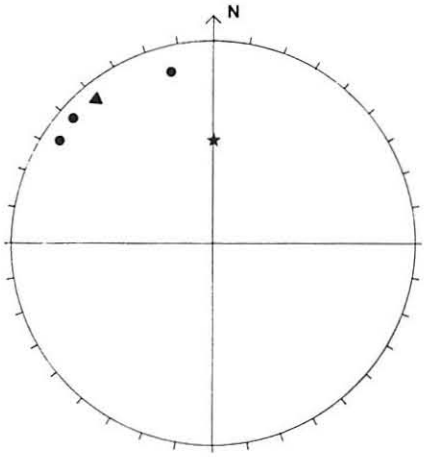

Text-fig. 11 Schmidt's equal-area projection of mean magnetization directions from sites PA3, PA4(A) and PA5(A) after thermal treatment at 300°C, before bedding correction (circles). Triangle — the mean of the three sites. Data are given in Table 2.

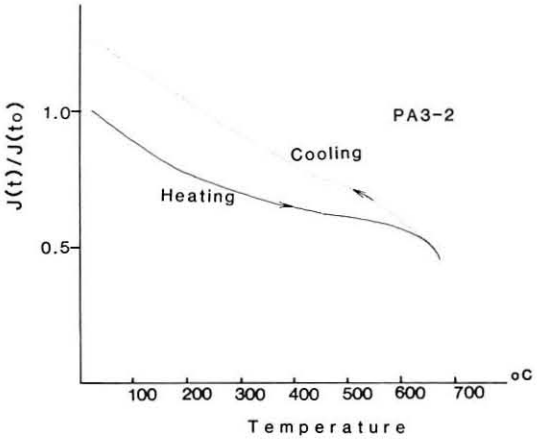

Text-fig. 12 Thermomagnetic curve for a specimen (purple slate) PA3-2 from Ramdighat Formation. Applied Field = 2400 Oe.

The mean directions for 3 sites belonging to the Ramdighat Formation yield a mean-site with NNW declination and shallow downward inclination (Text-fig. 11). There is no improvement in the grouping of the directions after bedding correction (Table 2). Thermomagnetic curve of the purple slate specimen (Text-fig. 12) indicates hematite as the carrier of remanence. Microscopic examination of the specimens showed the distribution of larger part of opaque minerals (mainly hematite) along the cleavage rather than along the primary laminations. These facts favour the secondary nature of the revealed magnetization. The inclination (before bedding correction) suggests a shallow northern paleolatitude (5°N) of acquisition. This direction may be correlatable with the well reported "Collision component" observed in other parts of the Himalaya (e.g., in Tibetan Sedimentary Series, Nepal Himalaya, Klootwijk & Bingham, 1980).

The site-mean directions from Kerabari area show an improvement in grouping after bedding correction suggesting positive fold test. If the directions from two sites PA36 and PA37 are discarded (the directions are based on only 2 specimens in each site and the rocks in these sites are structurally highly disturbed because of their closeness to the MBT), the remaining 3 sites yield better grouping (Table 2, Text-fig. 13). The virtual geomagnetic pole position is calculated from this direction on the assumption that it represents characteristic direction (Table 3.). Given the scarcity of data and the weak magnetization of the rocks considered, this magnetization may not represent the accurate pole position. Furthermore, one single pole from the Early Paleozoic (?) and lack of previous paleomagnetic data from the Lesser Himalayan rocks in the region for the specified age range does not enable the author to elaborate the tectonic history of the area.

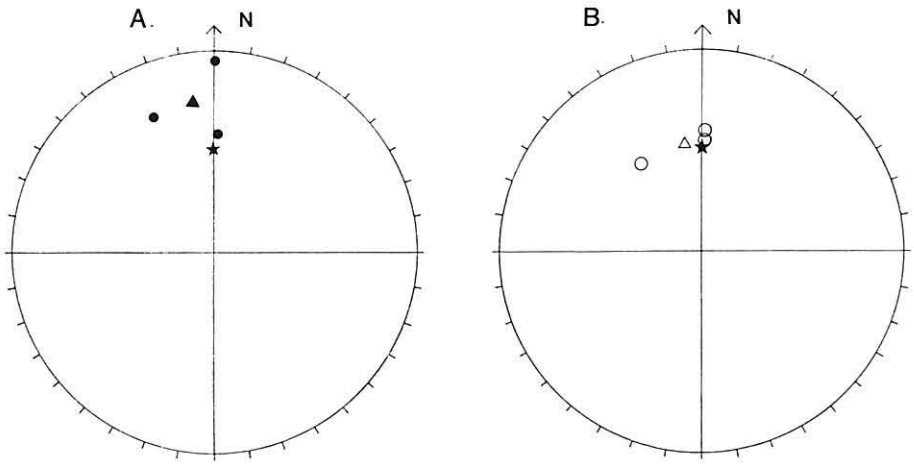

Text-fig. 13 Schmidt's equal area projection of mean magnetization directions from sites PA38, PA39 and PA40 after cleaning at 300 Oersted peak field. **A.** before bedding correction, **B.** after bedding correction. Triangle — the mean of three sites. Star — dipole field direction, as before.

Table 3 Virtual geomagnetic pole position of Kerabari Formation

Location		Mean direction			South pole position				Paleolatitude
lat. (°N)	long. (°E)	D_c (°)	I_c (°)	a_{95} (°)	lat. (°S)	long. (°E)	dp (°)	dm (°)	(°S)
27.7	83.5	350	−45	15	36	95	11	18	27

dp and dm are the semi-axes of the oval of 95% confidence of the pole positioin.

Conclusions

The following conclusions are drawn on the basis of the results of preliminary paleomagnetic investigations of Kali Gandaki Supergroup rocks from Tansen area:

(1) Most of the rocks are magnetically weak with their intensity of 10^{-7} order, in emu/cc. The NRMs of these rocks represent either complete or partial overprinting in the recent geomagnetic field. Application of AF (up to 530 Oe) or TH demagnetization can not unveil the primary magnetic component either because of the rapid decay of the intensity to the instrument noise level after a few cleaning steps or owing to the presence of very hard secondary recent field component.

(2) The purple slate rocks from Ramdighat Formation and carbonates from Kerabari formation are likely suitable for further paleomagnetic research. The former can be easily measured because of their higher intensities although the magnetization is believed to be of secondary origin, while the latter seem to possess primary magnetization which can be determined after AF cleaning treatment though they are relatively weakly magnetized. However, an extensive sampling coverage with collection of several samples from each site is needed to get meaningful data.

Acknowledgments

The author is highly grateful to Dr. Y. Fujiwara, Hokkaido University, for his continuous guidance during the paleomagnetic research. He wishes to thank Dr. M. Yoshida who kindly guided in the field during sampling and constantly encouraged during this study. Sincere thanks are extended to Prof. M. Kato, Hokkaido University and Dr. M.P. Sharma, Tribhuvan University for their constant encouragement to him during the course of this study.

This research work became possible due to Mombusho (Ministry of Education, Japan) Research Student Scholarship granted to the author for research at Hokkaido University for which he is highly indebted. He is grateful to the JOCV (Japan Overseas Cooperation Volunteers) office, at Kathmandu, for partial financial support during field work.

References

Arita, K., Hayashi, D. and Yoshida, M., 1982. Geology and structure of the Pokhara-Piuthan area, Central Nepal. *Jour. Nepal Geol. Soc.*, 2, Special issue: 5-30.

Arita, K. and Yoshida, M., 1982. Geological observations along motor road from Butwal to Ramdighat, Central Nepal. *Jour. Nepal Geol. Soc.*, 2, Special issue: 51-58.

Bingham, D.K. and Klootwijk, C.T., 1980. Palaeomagnetic constraints on Greater India's underthrusting of the Tibetan Plateau. *Nature*, vol. 284: 336-338.

Collinson, D.W., 1983. *Paleomagnetism. Techniques and instrumentation.* Chapman & Hall, London 502pp.

Frank, W. and Fuchs, G.R., 1970. Geological investigations in west Nepal and their significance for the geology of the Himalayas. *Geol. Rdsch.*, 59: 552-580.

Fuchs, G.R., 1980. The Lesser Himalayan geology of West Nepal and its regional importance. In: K.S. Valdiya and S.K. Bhatia (Editors), *Stratigraphy and correlations of Lesser Himalayan formations.* Hindustan Publishing Corp., Delhi: pp. 163-173.

Fuchs, G.R. and Frank, W., 1970. The Geology of West Nepal between the rivers Kali Gandaki and Thulo

Bheri. *Jahrb. Geol. Bundesanst.*, 18: 103pp.

Hashimoto, S., Ohta, Y. and Akiba, Ch. (Editors), 1973. *Geology of the Nepal Himalayas*. Saikon Publ., Tokyo, 292pp.

Irving, E., 1964. *Paleomagnetism and its application to geological and geophysical problems*. John Wiley and Sons, New York, 399pp.

Khramov, A.N. and Sholpo, L.E., 1967. *Paleomagnetism. Principles, methods and geological applications of paleomagnetology* (in Russian). Nedra publ., Leningrad, 252pp.

Klootwijk, C.T. and Bingham, D.K., 1980. The extent of Greater India, III. palaeomagnetic data from the Tibetan Sedimentary Series, Thakkhola region, Nepal Himalaya. *Earth and Planetary Science Letters*, 51: 381-405.

Mascle G.H., 1980. Tectonic reconstruction of stratigraphy of Midland in Central Nepal in the light of structural analysis. In: K.S. Valdiya and S.K. Bhatia (Editors), *Stratigraphy and correlations of Lesser Himalayan formations.* Hindustan Publishing Corp., Delhi: pp.191-197.

Sakai, H., 1983. Geology of the Tansen Group of the Lesser Himalaya in Nepal. *Mem. Fac. Sci., Kyushu Univ.*, ser. D, Geol., Vol. xxv, 1: 27-74.

Sakai, H., 1984. Stratigraphy of Tansen area in the Nepal Lesser Himalayas. *Jour. Nepal Geol. Soc.*, 4, Special issue: 53-61.

Sakai, H., 1985. Geology of the Kali Gandaki Supergroup of the Lesser Himalayas in Nepal. *Mem. Fac. Sci., Kyushu Univ.*, ser. D, Geol., vol. xxv, 3: 337-397.

Sharma, C.K., 1980. Stratigraphy of Lesser Himalayan formations of Western Nepal. In: K.S. Valdiya and S.K. Bhatia (Editors), *Stratigraphy and crrelations of Lesser Himalayan formations*. Hindustan Publishing Corp., Delhi: pp.174-179.

Sharma, T., Kansakar, D.R. and Kizaki, K., 1984. Geology and Tectonics of the region between Kali Gandaki and Bheri rivers in Central West Nepal. *Bull. College of Science, Univ. of the Ryukyus*, 38: 57-102.

Tokuoka, T. and Yoshida, M., 1984. Some characteristics of the Siwalik (Churia) Group in Chitwan Dun, Central Nepal. *Jour. Nepal Geol. Soc.*, 4, Special issue: 101-120.

Yamanaka, H., Yoshida, M. and Arita, K., 1982. Terrace landform and Quaternary deposit around Pokhara valley, Central Nepal. *Jour. Nepal Geol. Soc.*, 2, Speical issue: 113-142.

Yoshida, M. et. al., 1984. Magnetostratigraphic and pollen analytic studies of the Takmar Series, Nepal Himalayas. *Jour. Nepal Geol. Soc.*, 4, Special issue: 101-120

Yoshida, M. and Igarashi, Y., 1984. Neogene to Quaternary lacustrine sediments in the Kathmandu valley, Nepal. *Jour. Nepal Geol. Soc.*, 4, Special issue: 73-100.

Yoshida, M. and Sakai H., 1984. Some observations on the Paleomagnetism of Tansen Group, West Central Nepal. *Jour. Nepal Geol. Soc.*, 4, Special issue: 53-61.

Zijderveld, J.D.A., 1967. A.C. Demagnetization of rocks: Analysis of results. In: D.W. Collinson, K.M. Creer and S.K. Runcorn (Editors), *Methods in Paleomagnetism*. Elsevier, Amsterdam, pp.254-286.

(Manuscript received on October 21, 1986, and accepted on November 10, 1986)